Mott Insulating $S = 1$ Magnet in Quasi-One-Dimensional Vanadium Sublattice

One-dimensional materials remain an active topic of research because of their unique properties and potential electrical applications.[1] Calvagna *et al.* reported the crystal structure of sulfide oxide $Ba_3V_2S_4O_3$ and the band structure calculations.[2] This material which consists of *quasi*-1D vanadium sub-lattices was rarely suggested to be metallic. For example, the formally isovalent $BaVS_3$, also containing a 1D vanadium-sulfur structure, is a well studied system that exhibits a metal-insulator transition.[3] For insulating spin systems, 1D transition-metal sublattices can be of great interest to physicists, as Haldane gaps can be found in integer spin systems and Luttinger liquid phenomena in $S = 1/2$ systems.[4,5] Transition-metal sulfide oxides are also of interest due to their possible applications and ability to form anionic superlattices that result in atypical properties. Charge disproportionation according to the hard-soft acid-base (HSAB) rule is likely in superlattices with smaller (larger) cationic charges near softer (harder) anions. Many factors thus contribute to the potential interest in $Ba_3V_2S_4O_3$, but insufficient amounts of single-phase material have been synthesized. Hopkins *et al.*[6] synthesized single-phase $Ba_3V_2S_4O_3$, studied its transport and magnetic properties and clarified the underlying V 3d electronic structures.

Figure 1 shows the crystal structure of $Ba_3V_2S_4O_3$. Face-sharing VS_6 octahedra construct one dimensional columns, which are separated by Ba atoms and VSO_3 tetrahedra. These tetrahedra clearly depict the polarity of the crystal structure, as all tetrahedral have sulfur pointing in the same direction.

As for the transport property, in contrast to predictions from calculations in previous work,[2] no metallic character is observed in the measurement of resistivity of $BaV_2S_4O_3$, shown in Fig. 2. For the magnetic properties, $BaV_2S_4O_3$ shows paramagnetic behaviour at high temperature as inverse magnetic susceptibility $\chi^{-1}(T)$ is linear, in the inset of Fig. 2. A Curie-Weiss fit of data measured between 300 and 750 K gives 2.77 μ_B per formula unit.

To clarify the underlying V 3d electronic structures of $BaV_2S_4O_3$, Hopkins *et al.* measured V $L_{2,3}$-edge soft X-ray absorption spectroscopy (XAS) of $Ba_3V_2S_4O_3$ at **BL08B1**. XAS were recorded in the total- electron-yield mode with photon-energy resolution 0.2 eV. Figure 3 presents V $L_{2,3}$-edge XAS of $Ba_3V_2S_4O_3$ (black line). Two weak spectral features about 513.1 and 513.6 eV bear a resemblance to those of V_2O_3, which means that V^{III} exists in the

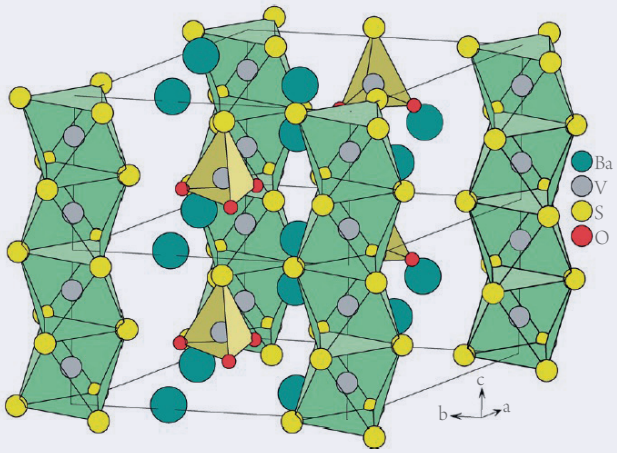

Fig. 1: Crystal structure of $Ba_3V_2S_4O_3$. [Reproduced from Ref. 6]

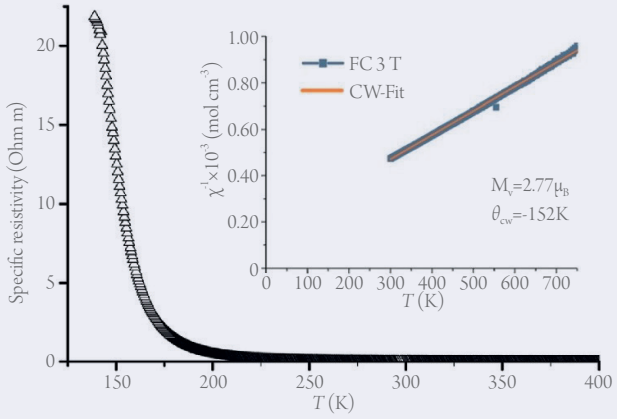

Fig. 2: Specific resistivity as a function of temperature. Inset shows the Curie-Weiss fit, calculated from the inverse magnetic susceptibility χ^{-1} at the highest temperatures. M_V is the magnetic moment per V^{III}. [Reproduced from Ref. 6]

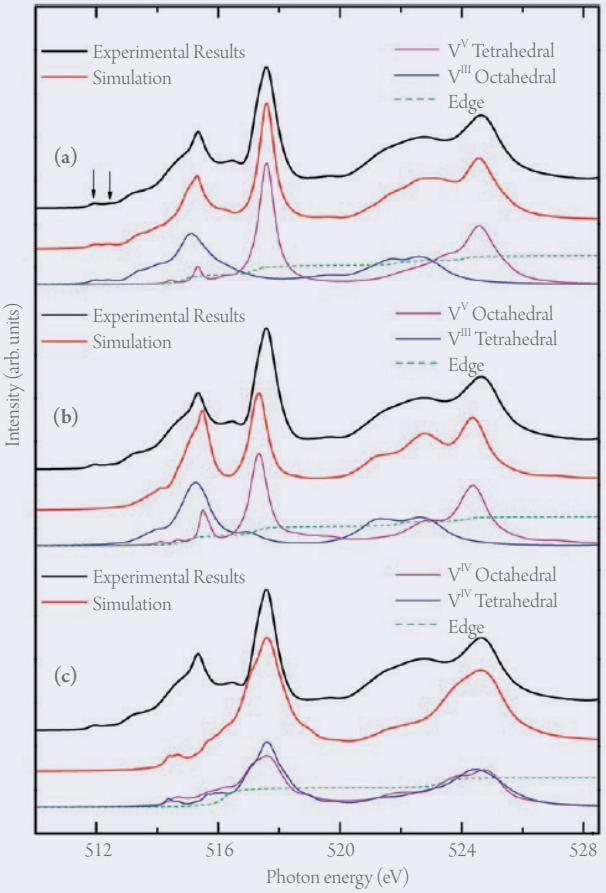

Fig. 3: Experimental V $L_{2,3}$-edge XAS (black line) of $Ba_3V_2S_4O_3$ and calculated spectra (red). The calculated spectra are the summations of the edge (green dashed line), V at tetragonal VO_3S and octahedral VS_6 sites (magenta and blue lines). (a) The tetrahedral site is V^V (magenta) and the octahedral site is V^{III} (blue). (b) Tetrahedral site V^{III} and octahedral site V^V. (c) Both sites are V^{IV}. In (a), the arrows indicate the typical features of V^{III} in an octahedron. [Reproduced from Ref. 6]

octahedral site, indicating a scenario in which V^{III} is in the octahedral VS_6 site and V^{V} is in the tetragonal VSO_3 site.

To confirm this mixed-valence state, they simulated the experimental spectrum of $Ba_3V_2S_4O_3$ with the well proven full-multiplet configuration-interaction approach (red line) using XTLS 8.3 code for three coordinations: (a) V^{III} in octahedral $V^{III}S_6$ site, V^{V} in tetragonal $V^{V}O_3S$ site, (b) V^{V} in octahedral $V^{V}S_6$ site and V^{III} in tetragonal $V^{III}O_3S$ site, and (c) both sites V^{IV}. Figure 3(a) shows a satisfactory agreement between the experimental spectrum (black line) and the theoretical simulation (red line). For $V^{V}S_6$ and $V^{III}O_3S$, Figure 3(b) shows a disagreement of overall spectral features of the experimental and simulated data, especially the lower-energy double signals about 513.1 and 513.6 eV originating from the V^{III} ion in the octahedral site. The possibility that both octahedral and tetrahedral sites have V^{IV} can also be excluded because of the disagreement of spectral features and the overall peak shape between the experimental results and simulation, shown in Fig. 3(c). These results clearly confirm the coordination $V^{III}S_6$ and $V^{V}O_3S$, a perfect example of charge disproportionation according to the HSAB rule; VIII is found purely with sulfur, that is, a soft anion, whereas the harder anion oxygen coordinates only to V^{V}. From the XAS, $Ba_3V_2S_4O_3$ contains one magnetic vanadium ion, V^{III} (d^2, $S = 1$), and one diamagnetic V^{V} (d^0, $S = 0$) per formula unit. The expected spin-only moment for a species with $S = 1$ is 2.83 μ_B, which is near the value 2.77 μ_B estimated from a Curie-Weiss fit of $\chi^{-1}(T)$ data.

Hopkins *et al.* synthesized a single-phase $Ba_3V_2S_4O_3$ powder, and investigated its physical properties. They clarified that vanadium in $Ba_3V_2S_4O_3$ takes charge-disproportionated $V^{III}S_6$ and $V^{V}SO_3$ coordination through analysis of XAS, which means that $Ba_3V_2S_4O_3$ is Mott insulating with $S = 1$. (Reported by Jun Okamoto)

This report features the work of Emily J. Hopkins, Zhiwei Hu, Liu Hao Tjeng and their co-workers published in Chem.-Eur. J. ***21****, 7938 (2015).*

References

1. C. Blumenstein, J. Schäffer, S. Mietke, S. Meyer, A. Dollinger, M. Lochner, X. Y. Cui, L. Patthey, R. Matzdorf, and R. Claessen, Nature Phys. **7**, 776 (2011).
2. F. Calvagna, J. Zhang, S. Li, and C. Zheng, Chem. Mater. **13**, 304 (2001).
3. M. Nakamura, A. Sekiyama, H. Namatame, and A. Fujimori, Phys. Rev. B **49**, 16191 (1994).
4. I. Affeck, J. Phys. Condens. Matter **1**, 3047 (1989).
5. F. D. M. Haldane, Phys. Rev. Lett. **45**, 1358 (1980).
6. B. J. Hopkins, Y. Prots, U. Burkhardt, Y. Watier, Z. Hu, C. Y. Kuo, J.-C. Chiang, T.-W. Pi, A. Tanaka, L.-H. Tjeng, and M. Valldor, Chem. Eur. J. **21**, 7983 (2015).

Three-Dimensional Dirac Semimetal

Topological insulators (TI) are new quantum materials characterized with a bulk insulating gap and gapless surface states protected by time-reversal symmetry, which is realized by band inversion induced by spin-orbit coupling with an odd number of Dirac cones. The topological classification of materials has recently been extended to a higher dimension in the so-called three-dimensional topological Dirac semimetal (TDS) phase. In contrast to TI, the TDS phase exhibits linear dispersion in all three dimensions and is protected by the crystalline symmetry. A TDS phase was predicted theoretically in Na_3Bi and Cd_3As_2 materials and confirmed experimentally using angle-resolved photoemission spectroscopy (ARPES). These TDS phases might, notably, be a 3D-Dirac semimetal of a new type due to the lack of inversion symmetry, which causes the lifting of the spin degeneracy of certain bands in the vicinity of the Dirac point, thereby raising the possibility of realizing the Weyl semimetal phase. The 3D Dirac semimetal has thus attracted much attention in physics and material science. The conduction and valence bands of Cd_3As_2 touch at the Dirac nodes in the bulk band structure, which gives rise to bulk Dirac fermions featuring robust topologically protected linear dispersion in 3D. In 2015, a research team of Fang-Cheng Chou (National Taiwan University) demonstrated a method of growth to obtain large plate-like single crystals of Cd_3As_2 and performed various characterizations on a Cd_3As_2 single crystal to reveal its unique functionalities.

In their work, they presented a detailed report on the self-selecting vapor growth technique of the crystal growth and the characterization of large and high-quality single crystals of Cd_3As_2. In particular, they generated crystals containing self-selected large facets of two types, namely the (112) and (even 00) orientations. Figure 1 shows the X-ray diffraction pattern of the sample as grown and the refined synchrotron X-ray diffraction pattern recorded at **BL01C2**. All diffraction signals can be indexed with space group I41cd. A Rietveld refinement on the XRD pattern yields lattice parameters $a = 12.6512(3)$ Å and $c = 25.4435(4)$ Å. The crystal structure of Cd_3As_2 has been shown to be complicated, depending strongly on the temperature of growth and the rate of quenching. Two space groups have been assigned to the

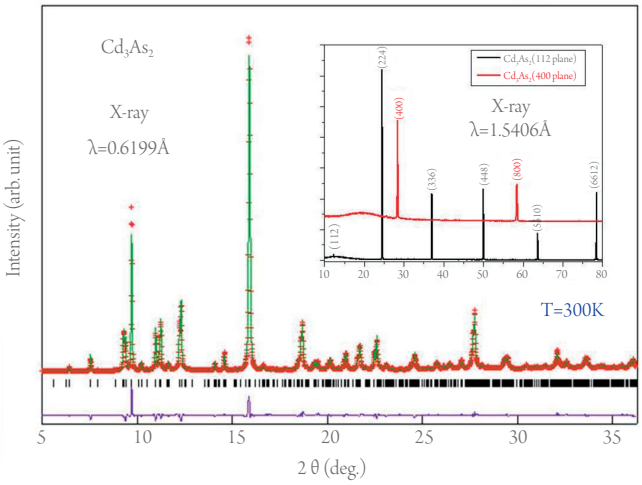

Fig. 1: Powder X-ray diffraction pattern of a Cd_3As_2 sample (red crosses) and its Rietveld refinement (green curve). The inset shows the obtained diffraction patterns of single crystals with facets of preferred orientations along directions (112) and (even 00).